International Journal of Natural and Engineering Sciences 8 (1): 53-60, 2014
ISSN: 1307-1149, E-ISSN: 2146-0086, www.nobel.gen.tr

Efficient Algorithms for Palmprint Identification Based on Non-linear Feature Extraction and Contourlet Transform

Ali YOUNESI* Mehdi Chehel AMIRANI
Department of Electrical Engineering, Urmia University, Urmia, Iran

*Corresponding author:
Email: st_a.yonesi@urmia.ac.ir

Received: April 03, 2014
Accepted: May 09, 2014

Abstract
One of robust biometrics is palmprint. Feature extraction from palm area is an important issue and can determine the complexity and efficiency of identification system. In this paper, we propose a new method to extract region of interest (ROI) and two efficient algorithmsfor feature extraction from palmprint. The first algorithm calculates isometric projection (IsoP) of ROI and the second one calculates the gray-level co-occurrence matrix (GLCM) of contourlet sub-bands of ROI to extract raw features. In both algorithms linear discriminant analysis (LDA) is used to select proper features from raw extracted features and then,K-nearest neighbor (KNN) and support vector machine (SVM) classifiers are used to identify person. Hong Kong Polytechnic University (PolyU) palmprint database is used to evaluate the performance of the proposed algorithms. Experimental results on 200 different persons demonstrate that the proposed methods have better efficiency in comparison with recently proposed algorithms for palmprint identification.
Keywords: Contourlet; GLCM; IsoP; KNN; LDA; Palmprint; SVM.

INTRODUCTION

Recently, to provide higher level of security to personal identification systems, biometrics has been considered as a reliable technology. Among the various biometric characteristics that can be used to recognize a person, the human hand is the oldest, and perhaps the most successful form of biometric technology [1]. The features that can be extracted from the hand include hand geometry, fingerprint, palmprint, knuckle print, and vein. These hand properties are stable and reliable. If the age of person increases, the hand structure and configuration remain relatively stable throughout the person's life [2]. Apart from that, the hand-scan technology is generally perceived as non-intrusive as compared to iris or retina-scan systems [3]. The users do not need to be aware of the way in which they interact with the system. These advantages have greatly facilitated the deployment of hand features in biometric applications. In comparison with fingerprint and hand geometry, palmprint contains more rich information, so they are more distinctive. Also, palmprint is easily captured even with lower resolution devices, which would be cheaper. By capturing palmprint, all palm features such as hand geometry, minutiae features, principal and wrinkles could be combined to build a more accurate and robust multi-modal biometric system.

Feature extraction from palm area is critical step in palmprint identification. There are many researches which performed for palmprint identification. In general, there are two types of features that used in these systems; statistical and structural features [4]. From first category, we can mention eigen-palm [5], fisher-palm [6], Fourier transform [7], Gabor filter [8], and wavelet transform [9]. Principal lines, creases, delta points, minutiae [10-12] are listed in structural features.Chen et al. [13] have used contourlet transform and AdaBoost in their system. Lu et al. [14] proposed a palmprint recognition method based on the eigen-space techniques where the original palmprint images were transformed by the Karhoenen-Loeve transformation with the obtained eigen-palm features used for palmprint recognition. In [15] multiple templates matching via the correlation function and the back-propagation neural network was used for verification and identification. Dai et al. [16] applied *M*-band wavelets and used the 1-norm texture energy as the feature vectors for image representation. Also, texture-based analysis is more powerful utility to extract image representation features for classification. For example, Gabor filters can be applied to either the whole palm or the specific palm regions to extract the texture changes of the palm. Due to their superior performance, many works have focused on using the Gabor wavelet representations [17-19]. Because of most benefits of texture-based features, this type of features are used in this paper.

All palmprints are acquired by hand scan device are not suitable for identification. So at first region of interest (ROI) must be extracted from palmprint to reduce redundancy from palmprint image. In this paper, we present a new method for ROI extraction based on center of mass of palmprint image. Proposed method has low complexity and is a robust method for ROI extraction.

Isometric projection (IsoP) [20] is used to construct primary feature vector from ROI in the first algorithm. IsoP is a nonlinear approach for feature extraction. Contourlet transform [21] is an efficient tool for extraction of smooth contours by using multi-scale and directional filter banks. Therefore, in the second algorithm this transform is applied on ROI to extract contours. Depending on number of decomposition levels, some sub-bands are extracted. The gray-level co-occurrence matrix (GLCM) [22] is a method for extracting second order statistical texture features. Therefore, GLCM of each sub-band is calculated to develop feature vector.

All raw extracted features are not suitable and feature conditioning must be performed to reduce the dimensionality of the raw feature vector. For this purpose, linear discriminant analysis (LDA) [23] is used. After feature conditioning, extracted proper features must be classified to palmprint identification. Support vector machine (SVM) [23] and K-nearest neighbor (KNN) [23] are efficient classifiers that used widely in classification-based systems. Efficiency of proposed system is measured by means of correct classification rate (CCR).Hong Kong Polytechnic University (PolyU) palmprint database [24] is a widely used database in palmprint identification literature. We select this database to evaluate the performance of proposed system. Experimental results on 200 different palms from this database indicate the robustness of proposed algorithms in palmprint identification.

The rest of this paper is organized as follows. Section II describes the details of proposed palmprint identification system. Section III contains database description and results. Finally, Section IV concludes this paper.

ProposedMethods for Palmprint Identification

Fig. 1 presents the block diagram of proposed palmprint identification system. The first step is palmprint image acquisition. In this paper, palmprint images are acquired from PolyU database as the more previous researches. In the next, other steps are explained in more details.

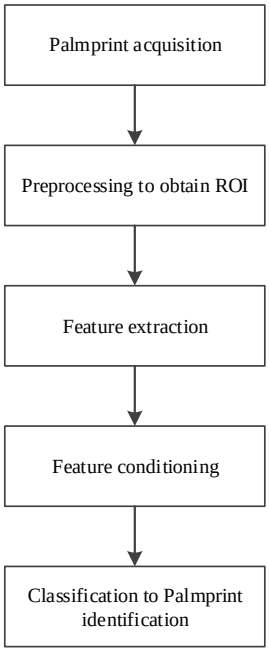

Fig. 1. Block diagram of the proposed palmprint identification algorithm.

Preprocessing to obtain ROI

Some images from PolyU database are shown in Fig. 2. Background of all images has very low intensity values. So, it is clear whole of palmprint image are not suitable for identification. Previous researches have showed that most significance part of palmprint is in the center of palmprint. Therefore, at first significance part of palmprint must be extracted.

In this paper, we propose a new method for ROI extraction. Different steps of proposed method are shown in Fig. 3. In PolyU database, background is not complex and has uniform black color. So, one optimum threshold value can extract palm area from background. We obtain this optimum threshold value by *Otsu*'s method [25]. So, gray-scale palmprint is converted to binary palmprint by following approach.

$$P_{Bin}(x,y)=\begin{cases}1 & \text{if } P_{Gray}(x,y)>Th \\ 0 & \text{Otherwise}\end{cases} \quad (1)$$

where P_{Bin} is binary palmprint, P_{Gray} is original gray-scale palmprint, and Th is the optimum threshold value. Original gray-scale palmprint and corresponding binary palmprint are shown in Fig. 4a and Fig. 4b, respectively. Lighting conditions can cause that some palm regions don't appear in binary image. To overcome this problem, we perform morphological closing operation [25] with disk structure element on primary binary image (P_{Bin}). Morphological closing operation consists of two morphological operations; i.e., dilation and erosion. This operation is described as following.

$$P_{Bin,close}=((P_{Bin}\oplus Se)\ominus Se) \quad (2)$$

where P_{Bin} is original binary image, $P_{Bin,close}$ is the result of closing and Se is the structure element. Also, $\oplus$ and $\ominus$ denote dilation and erosion operators, respectively. At first, image is dilated by structure elementSe and then dilated image is eroded by the same structure element. The resulting image is shown in Fig. 4c. As seen, sometimes other unwanted regions appear in binary image. To remove them, we remain biggest connected component and remove the others. Result is shown in Fig. 4d.

To find ROI, we propose to find center of mass of connected component related to palm area. Center of mass is defined as

$$\begin{cases}C(x)=\frac{1}{N}\sum_{i\in B}x(i) \\ C(y)=\frac{1}{N}\sum_{i\in B}y(i)\end{cases} \quad (3)$$

where $C(x)$ and $C(y)$ denote the location of center of mass in x-axis and y-axis, respectively. Location of white pixels that belong to palm connected component (B) is determined by (x, y), and N is number of white pixels belong to B. Center of mass of palm area is shown by red dot in Fig. 4e. In order to determine the boundary of ROI, at first we determine width of ROI. For this purpose, as shown in Fig. 4e, the distance between two border points (L and R) in y-axis denoted as $D_w$is calculated as

$$D_w=L(y)-R(y) \quad (4)$$

where $L(y)$ and $R(y)$ denote the location of left and right boundary points (L and R) in y-axis. Based on our experiments, location of L_f and R_f points that determines the width of ROI is calculated as

$$\begin{cases}L_f(y)=L(y)+0.15D_w \\ R_f(y)=R(y)-0.15D_w\end{cases} \quad (5)$$

Fig. 2. Some palmprints from PolyU database.

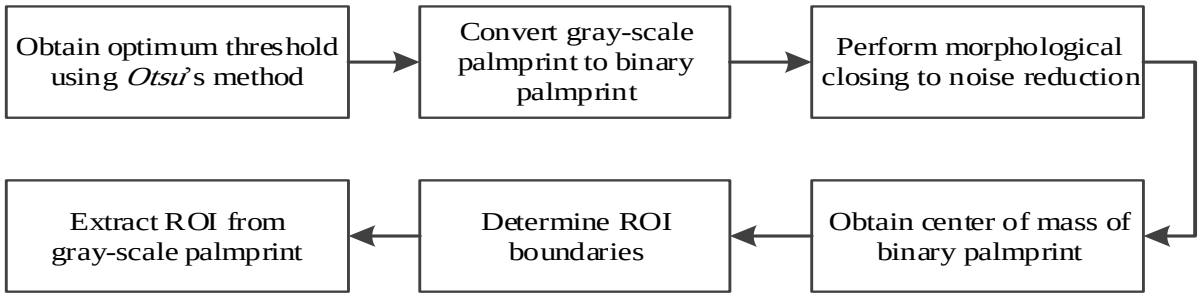

Fig. 3. Steps of the proposed ROI extraction from palmprint.

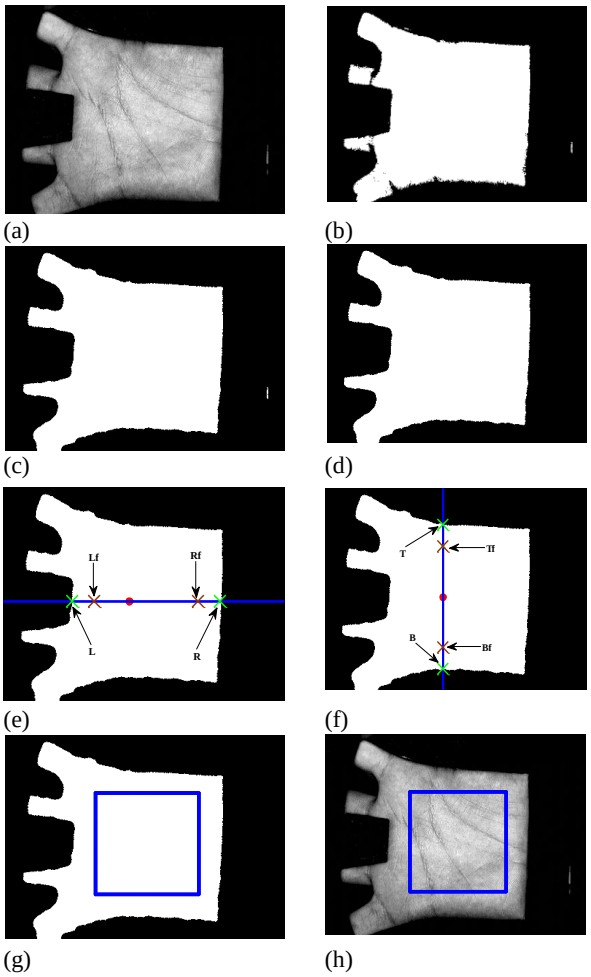

Fig. 4. Different steps for ROI extracting. **(a)** Original gray-scale palmprint, **(b)** primary binary image after applying *Otsu*'s threshold value, **(c)** binary image after closing, **(d)** binary image after selecting biggest connected component, **(e)** determine the left and right boundary of ROI, **(f)** determine the top and bottom boundary of ROI, **(g)** ROI in binary image, **(h)** ROI in original gray-scale palmprint.

shown in Fig. 4e. In order to find the boundary of ROI in the top and bottom of ROI, two border points (*T* and *B*) are found as shown in Fig. 4f. Then, distance between them (D_h) calculated as

$$D_h = B(x) - T(x) \qquad (6)$$

where $B(x)$ and $T(x)$denote the location of bottom and top border points (*B* and *T*) in x-axis. Finally, based on our experiments, the boundary points of ROI in the top and bottom ($B_f(x)$ and $T_f(x)$) are calculated as

$$\begin{cases} T_f(x) = T(x) + 0.15D_h \\ B_f(x) = B(x) - 0.15D_h \end{cases} \qquad (7)$$

These points determine the height of ROI that is shown in Fig. 4f. These four points i.e., $L_f(\mathrm{y})$, $R_f(\mathrm{y})$, $T_f(\mathrm{x})$, $B_f(x)$, determine the boundary of the ROI, and using these four points the ROI can be obtained as shown in Fig. 4g and Fig. 4h.

Feature Extraction

In this part, we describe two proposed algorithms for feature extraction from ROI. First method uses Isometric projection (IsoP) and second method uses combination of contourlet and GLCM.

Isometric projection

IsoP is non-linear unsupervised approach for data dimensionality reduction [20]. The classical techniques for dimensionality reduction, principal component analysis (PCA) and multidimensional scaling (MDS), are simple to implement, efficiently computable, and guaranteed to discover the true structure of data lying on or near a linear

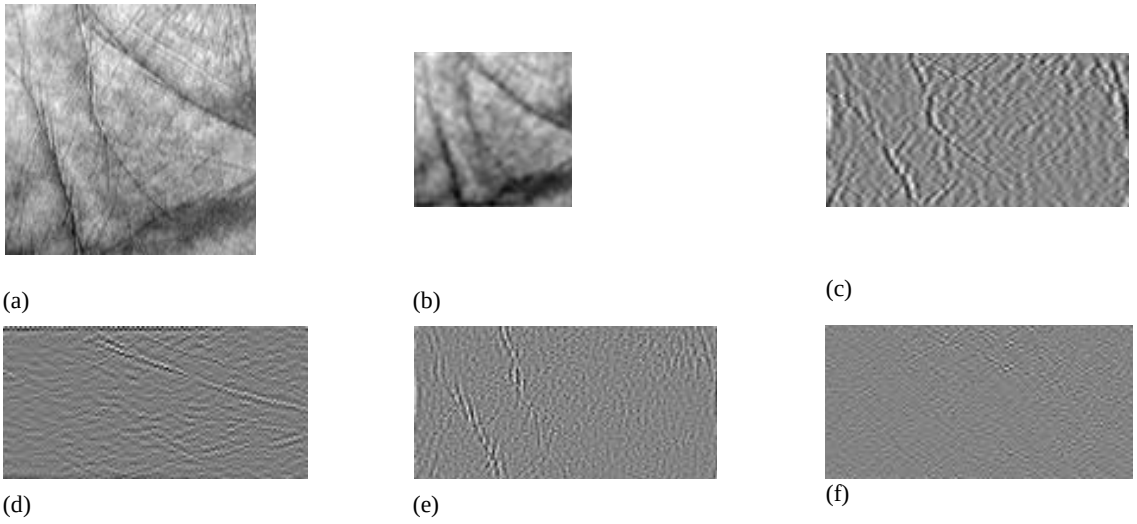

Fig. 5. Representation sub-bands of contourletSD transform. **(a)** ROI of palmprint,**(b) - (f)** Different sub-bands calculated by contourletSD.

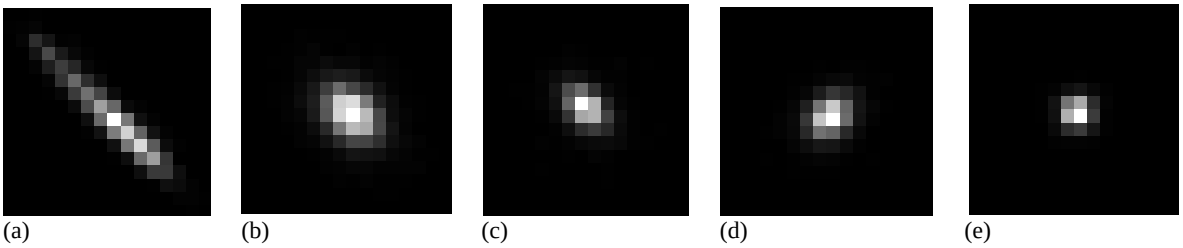

Fig. 6. GLCM of different sub-bands. (a) - (e) GLCM of sub-bands shown in Figs. 5b-5f.

subspace of the high-dimensional in input space [26]. The goal of PCA is to finds a low-dimensional of data points that best preserves their variance as measured in the high-dimensional input space. Classical MDS finds low-dimensional data that preserves the inter-point distances. However, many data sets contain essential non-linear structures that are invisible to PCA and MDS. IsoP is an approach that combines the major algorithmic features of PCA and MDS, such as computational efficiency and global optimality.

To dimensionality reduction, at first distances $d_X(i,j)$ between all pairs *i, j* from *N* data points in the high-dimensional input space *X*, measured either in the standard Euclidean metric or some domain-specific metric. Then in three steps IsoP reduces the dimensionality of data points as following.

- IsoP at first construct neighborhood graph. It defines the graph *G* over all data points *i* and *j* if (as measured by $d_X(i,j)$) they are close than ε_{IsoP} (ε_{IsoP} is the threshold distance to consider two points as neighbor) or if *i* is one of k_{IsoP} nearest neighbors of *j*. Set edge lengths equal to $d_X(i,j)$.
- Shortest paths are calculated as follows. $d_G(i,j)$ is constructed as

$$\begin{cases} d_X(i,j) & \text{if } i,j \text{ are linked by an edge} \\ \infty & \text{Otherwise} \end{cases} \quad (8)$$

Then for each value of $k = 1,...,N$ it turn, replace all entries $d_G(i,j)$ by

$$\min\left(d_G(i,j),\ d_G(i,k)+d_G(k,j)\right) \quad (9)$$

The matrix of final values $D_G = \{d_G(i,j)\}$ will contain the shortest path between all pairs of points in *G*.

- Finally, *d*-dimensional embedding is constructed. Let λ_p be the *p*th eigenvalue in descending order of the matrix $\tau(D_G)$ and V_p^i be the*i*th component of the *p*th eigenvector. The operator $\tau(D)$ is defined as

$$\tau(D) = -HSH/2 \quad (10)$$

where*S* is the matrix of squared distances i.e., $S_{i,j} = D_{i,j}^2$ and *H* is the centering matrix [26] calculated as

$$H_{i,j} = \delta_{i,j} - 1/N \quad (11)$$

Then *p*th component of the *d*-dimensional coordinate vector is obtained as

$$y_i = \sqrt{\lambda_p} V_p^i \quad (12)$$

The dimension of new space is determined according to the eigenvalues which will presents in the next section.

Contourlet transform and GLCM

The contourlet transform proposed by Do et al. [21] is a new two-dimensional extension of the wavelet transform using multi-scale and directional filter banks to overcome limitation of wavelets. At first, point's discontinuities captured into linear structure by Laplacian pyramid (LP) that constructed in double filter bank structure. The contourlet construction allows for any number of directional filter banks (DFB) decomposition levels l_j to be applied at each LP *level*$_j$.

The new contourlet transform with sharp frequency localization was presented in [27] which named contourletSD. Therefore, we use contourletSD transform in this paper. For directional and multi-scale decomposition steps, *pkva* and *raised cosine* filters are used, respectively. We use two levels of pyramidal decomposition and in each level the number of directional decomposition is equal to one. Using this decomposition levels, five different sub-bands are obtained. These sub-bands are shown in Fig. 5. In order to extract features from sub-bands of contourletSD, we calculate the GLCM of each sub-band. GLCM is calculated how often a pixel with a certain intensity I_i occurs in relation with another pixel I_j at a certain distance d_p and orientation θ [22]. In this paper, GLCM of each sub-band is calculated with 16 different gray-levels with d_p and θequal to 0. In Fig. 6, GLCM of each sub-band is presented.

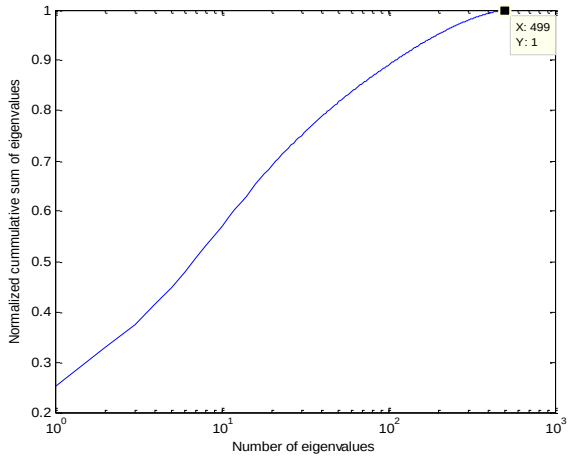

Fig. 7. Normalized cumulative sum of eigenvalues versus number of eigenvalues for IsoP.

Feature conditioning

LDA is a linear supervised algorithm for data dimensionality reduction. Because of supervised nature of LDA, it can generate feature vectors with low dimensionality [23]. The goal of LDA is decrease within-class distance and increase the between-class distance by combination matrix (W_{LDA}). These distances are defined as below. In order to achieve this goal, within-class (S_w) and between-class (S_b) scatter matrices are calculated according to

$$S_w = \sum_{i=1}^{M} P_i S_i \qquad (13)$$

where M is the number of classes and

$$\begin{cases} S_i = E\left[\left(\underline{x} - \underline{\mu}_i\right)\left(\underline{x} - \underline{\mu}_i\right)^T \right] \\ P_i \equiv P(\omega_i) \approx \dfrac{n_i}{N_{train}} \end{cases} \qquad (14)$$

wheren_i is training samples in class ω_i and $N_{train}$is number of total train vectors. Between-class scatter matrix is calculates as

$$S_b = \sum_{i=1}^{M} P_i \left(\underline{\mu}_i - \underline{\mu}_0\right)\left(\underline{\mu}_i - \underline{\mu}_0\right)^T \qquad (15)$$

where

$$\underline{\mu}_0 = \sum_{i=1}^{M} P_i \underline{\mu}_i \qquad (16)$$

In order to generate combination matrix (W_{LDA}), following criteria is defined.

$$\frac{\left| W_{LDA}^T S_b W_{LDA} \right|}{\left| W_{LDA}^T S_w W_{LDA} \right|} \qquad (17)$$

Finally, which W_{LDA} that maximizes (17) considered as combination matrix. Eigenvalues of the features determines the number of features selected by LDA which discussed in the next section.

RESULTS

Database description

In order to evaluate the performance of proposed algorithm, we use well-known Hong Kong Polytechnic University (PolyU) palmprint database [24], which is used is previous researches [13] and [28]. This database contains 7752 gray-scale images corresponding to 386 different palms in BMP image format. Around twenty samples from each of these palms were collected in two sessions, where around 10 samples were captured in each first and second sessions. The average interval between the first and the second collection was two months. The resolution of all the original palmprint images is 384×284 pixels at 75 dpi.

In this work, 200 different palms are chosen to evaluate the performance of the proposed methods. As [13] and [28] three palmprints of first session are used in training stage and remain palmprints are used is testing stage. Therefore, we use 600 images for system training and 3400 images for testing of system.

Performance of the first method

Feature space for all of palms must be equal. In [13] and [28], ROI is resized to 128×128 pixels. In first method, we resize all extracted ROIs to 32×32 pixels and by this approach we reduce the computational complexity. At first step feature extraction is performed using IsoP. According to size of ROI, 1024 features are given to IsoP algorithm. The eigenvalue of each feature vector demonstrates the relative amount of information in that feature. So, in order to feature extraction by IsoP, at first eigenvalue of features are calculated. In Fig. 7, normalized cumulative sum of

eigenvalues is shown (x-axis is shown in logarithmic scale).

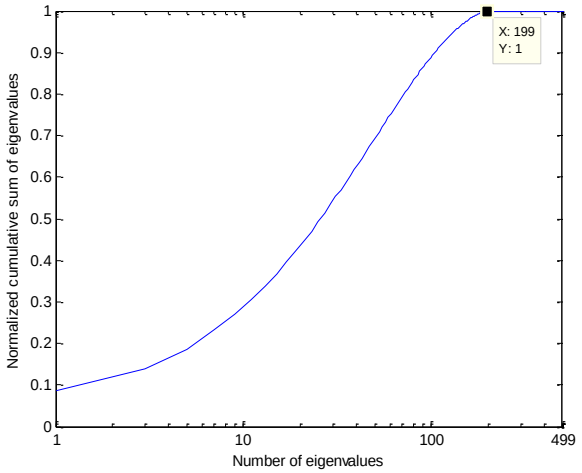

Fig. 8. Normalized cumulative sum of eigenvalues versus number of eigenvalues for LDA in the first method.

Since IsoP is unsupervised algorithm, so it can't embed information in the low dimensions. It is shown that 499 features contain about relative 100% information in feature vector. Therefore, 499 features are extracted by IsoP. Then, LDA is applied for feature conditioning. LDA is a supervised dimensionality reduction algorithm, so it is capable to embed most of information in low dimensions. For doing this, the normalized cumulative sum of eigenvalues of features that obtained by IsoP is calculated as shown in Fig. 8 (x-axis is shown in logarithmic scale). So, according to Fig. 7, 199 features are selected and the others are removed, which is significance reduction for dimensionality of primary features.

When proper features are selected from ROI, to individual identification, these features must be classified. K-nearest neighbor (KNN) and support vector machine (SVM) classifiers [23] are used for classification. These classifiers are popular and efficient classifiers that used in pattern recognition researches.

To determine the parameter of KNN classifier i.e., K, correct classification rate (CCR) for different values of K are calculated and presented in Table 1. The value of K that maximizes CCR is selected.As seen by increasing the value of K, CCR decreases. The maximum value of CCR is obtained for value of K equal to one. In this case the KNN classifier is the same as minimum distance classifier. The maximum CCR value obtained is 99.12%. SVMclassifier with radial basis function (RBF) kernel is used for classification. For this purpose *libSVM* toolbox [29] is used which is widely used in literatures. CCR is calculated for different combinations of effective parameters of SVMwith RBF kernel i.e., *C*and γ. The maximum CCR is obtained for $C = 2^4$ and $\gamma = 2^{-1}$ equals to 99.18% which is slightly better than CCR of KNN classifier in the first method.

Table 1. CCR versus different values of K using features obtained from first method

K	1	3	5	7	9	11
CCR (%)	99.12	99.06	99	98.94	87.06	80.00

Performance of the second method

At first ROI of all palmprints are resized to 128×128 pixels. Using this ROI, the size of sub-bands are obtained by contourletSD shown in Fig. 5 are 64×64, 64×128, 64×128, 64×128, and 64×128, respectively. According to 16 different gray-levels considered in constructing GLCM, the size of GLCM for each sub-band is equal to 256 (=16×16) and the size of primary features for each palmprint is 1280 (=5×256). But as seen in Fig. 6, most of GLCM values are zero. They must be removed from feature vector to reduce complexity and increase efficiency.

Normalized cumulative sum of eigenvalues of features is calculated as shown in Fig. 9 (x-axis is shown in logarithmic scale). So, according to Fig. 9, 199 features are selected and remove the others. Therefore, we reduce the feature dimensionality from 1280 to 199, which is significance reduction in dimensionality of primary features.

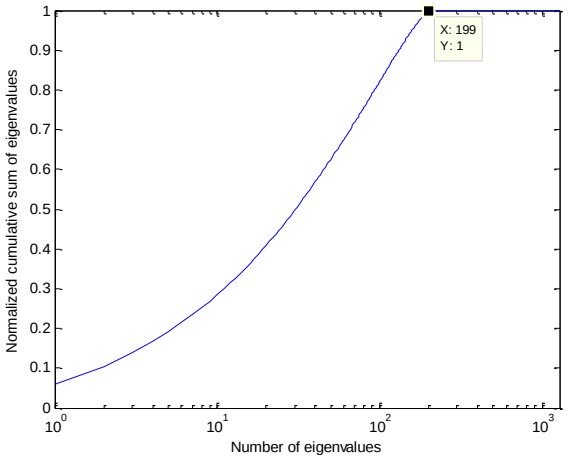

Fig. 9. Normalized cumulative sum of eigenvalues versus number of eigenvalues for LDA in the second method.

Achieved CCR for different values of the K for KNN classifier are presented in Table 2. As seen, by increasing the value of K, CCR reduces for the second method for feature extraction and as first method, K=1 achieves the maximum CCR equal to 99.26%. For SVM classifier, maximum CCR is obtained for $C = 2^{2.5}$ and $\gamma = 2^{0.5}$ equals to 99.47% which is better than CCR of KNN classifier in the first method.

Table 2. CCR versus different values of K using features obtained from second method

K	1	3	5	7	9	11
CCR (%)	99.26	99.12	98.97	98.53	91.18	85.29

As seen, second proposed method for feature extraction achieves better CCR for both classifiers than the first proposed method for feature extraction.

In Table 3, we compare the results of proposed method with recently proposed methods for palmprint identification. Chen et al. [13] have used contourlet transform and AdaBoost in their system. Meraoumia et al. [28] used Gaussian probability density function and two-dimensional block based discrete cosine transform (DCT).It is obvious that proposed algorithm has better efficiency than other methods.It should be mentioned that in [13] and [28] authors used 100 different palms and we use 200

different palms which is more than the [13] and [28], and we obtain better CCR than the previous works.

Table 3. Comparison between proposed method and other methods.

Method	CCR (%)
First proposed method (IsoP+PCA+LDA+SVM)	99.18
First proposed method (IsoP+PCA+LDA+KNN)	99.12
Second proposed method (Contourlet+GLCM+PCA+LDA+SVM)	99.47
Second proposed method (Contourlet+GLCM+PCA+LDA+KNN)	99.26
Method of [13]	99
Method of [28]	98.93

CONCLUSION

In this paper, two algorithms for palmprint identification based on IsoP and combination of contourletSD transform and GLCM were presented. At first, we introduced a robust method for ROI extraction from palmprint based on center of mass of palm area. Two different feature extraction methods were proposed. First method calculates the IsoP of the RIO, and in the second method contourletSD transform of ROI is calculated and then GLCM of each sub-band is computed. LDA was used for conditioning after feature extraction in both methods .Finally, well-known KNN and SVM with RBF kernel classifiers were used to personal identification. Experimental results were obtained using PolyUpalmprint database. Experimental results shown that SVM classifier has better performance than the KNN in both methods for feature extraction. Also, features obtained using GLCM of the contourlet transform has better personal identification rate for both classifiers in comparison with features obtained with IsoP.

REFERENCES

[1] Hand-based Biometrics, *Biometric Technology Today*, vol.11, no.7, pp. 9-11, 2003.

[2] E. Yoruk, H. Dutagaci, and B. Sankur, "Hand biometrics," *Image and Vision Computing*, vol. 24, no. 5, pp. 483-497, 2006.

[3] A. K. Jain, A. Ross, and S. Prabhakar, "An Introduction to biometric recognition," *IEEE Trans. Circuits System and Video Technology*, vol. 14, no. 1, pp. 4-20, 2004.

[4] T. Connie, A. Jin, M. Ong, and D. Ling, "An automated palmprint recognition system," *Image and Vision Computing*, vol. 23, pp. 501-515, 2005.

[5] G. Lu, D. Zhang, and K. Wang, "Palmprint recognition using eigenpalm features," *Pattern recognition Letters*, vol. 24, pp. 1463-1467, 2003.

[6] X. Wu, G. Lu, D. Zhang, and K. Wang, "Fisherpalms based palmprint recognition," *Pattern recognition Letters*, vol. 24, pp. 2829-2838, 2003.

[7] W. Li, D. Zhang, and Z. Xu, "Palmprint Identification by Fourier Transform," in *Proc. of Int'l Journal of Pattern Recognition and Artificial Intelligence*, vol. 16, pp. 417-432, 2002.

[8] W. Kong, D. Zhang, and W. Li, "Palmprint feature extraction using 2-D Gabor filters," *Pattern recognition*, vol. 36, pp. 2339-2347, 2003.

[9] L. Zhang and D. Zhang, "Characterization of palmprints by wavelet signatures via directional context modeling," *IEEE Trans. Man and Cybernetics*, vol. 34, pp. 1335-1347, 2004.

[10] D. Zhang and W. Shu, "Two novel characteristics in palmprint verification: datum point invariance and line feature matching," *Pattern Recognition*, vol. 32, pp. 692-702, 1999.

[11] J. Chen, C. Zhang, and G. Rong, "Palmprint Recognition using crease," in *Proc. of Int'l Conf. on Image Processing*, vol. 3, pp. 234-237, 2001.

[12] C. Han, H. Cheng, C. Lin, and K. Fan, "Personal authentication using palm-print features," *Pattern Recognition*, vol. 36, pp. 371-381, 2003.

[13] G. Y. Chen and B. K´egl, "Palmprint Classification using Contourlets," in *Proc. of IEEE Int'l Conf. on Systems, Man and Cybernetics*, pp. 1003-1007, 2007.

[14] G. M. Lu, D. Zhang, and K. Q. Wang, "Palmprint recognition using eigenpalms features," *Pattern Recognition Letters*, vol. 24, pp. 1463-1467, 2002.

[15] C. C. Han, H. L. Chen, C. L. Lin, and K. C. Fan, "Personal authentication using palm-print features," *Pattern Recognition*, vol. 36 no. 2, pp. 371-381, 2003.

[16] Q. Dai, N. Bi, D. Huang, D. Zhang and F. Li, "M-Band wavelets application to palmprint recognition based on texture features", in *Proc. of IEEE Int'l Conf. on Image Processing*, pp.893-896, 2004.

[17] W. Li, J. You, and D. Zhang, "Texture-based palmprint retrieval using a layered search scheme for personal identification," *IEEE Trans. Multimedia*, vol. 7, no. 5, pp. 891-898, 2005.

[18] S. Arivazhagan, L. Ganesan, and S. Priyal, "Texture classification using Gabor wavelets based rotation invariant features," *Pattern Recognition Letters*, vol. 27, no. 16, pp. 1976-1982, 2006.

[19] W. Kong, D. Zhang, and W. Li, "Palmprint feature extraction using 2-D Gabor filters," *Pattern Recognition*, vol. 36, no. 10, pp. 2339-2347, 2003.

[20] J. B. Tenenbaum, V. de Silva, and J. C. Langford, "A Global Geometric Framework for Nonlinear Dimensionality Reduction," *Science magazine*, vol. 290, pp. 2319-2323, 2000.

[21] M. N. Do and M. Vetterli, "The contourlet transform: an efficient directional multi-resolution image representation," *IEEE Trans. Image Processing*, vol. 14, no. 12, pp. 2091-2106, 2005.

[22] R. M. Haralick, K. Shanmugam, and I. Dinstein, "Textural features for image classification," *IEEE Trans. Systems, Man and Cybernetics*, vol. SMC-3, no. 6, pp. 610-621, 1973.

[23] S. Theodoridis and K. Koutroumbas, *Pattern Recognition*, Elsevier, 4th Edition, 2008.

[24] The Hong Kong Polytechnic University, PolyU Palmprint Database, [Online]. Available: *http:// www.comp.polyu.edu.hk/ biometrics.*

[25] R. C. Gonzalez and R. E. Woods, *Digital Image Processing*, Prentice Hall, 3rd Edition, 2008.

[26] K. V. Mardia, J. T. Kent, and J. M. Bibby, *Multivariate Analysis*, Academic Press, London, 1979.

[27] Y. Lu and M. N. Do, "A new contourlet transform with sharp frequency localization," in *Proc. IEEE Int'l Conf. on Image Processing*, pp. 1629-1632, 2006.

[28] A. Meraoumia, S. Chitroub, and A. Bouridane, "Gaussian modeling and discrete cosine transform for efficient and Automatic palmprint identification," in *Proc. of Int'l Conf. Machineand WebIntelligence*, pp. 121-125, 2010.

[29] Ch. Chang and Ch. Lin, LIBSVM: a library for support vector machines, 2001. Software available at *http://www.csie.ntu.edu.tw/~cjlin/libsvm*.